OPEN

Molecular Psychiatry (2014), 1–8

www.nature.com/mp

IMMEDIATE COMMUNICATION

Cortical fast-spiking parvalbumin interneurons enwrapped in the perineuronal net express the metallopeptidases Adamts8, Adamts15 and Neprilysin

J Rossier[1], A Bernard[2], J-H Cabungcal[3], Q Perrenoud[4], A Savoye[1], T Gallopin[4], M Hawrylycz[2], M Cuénod[3], K Do[3,5], A Urban[1,5] and Ed S Lein[2,5]

The *in situ* hybridization Allen Mouse Brain Atlas was mined for proteases expressed in the somatosensory cerebral cortex. Among the 480 genes coding for protease/peptidases, only four were found enriched in cortical interneurons: *Reln* coding for reelin; *Adamts8* and *Adamts15* belonging to the class of metzincin proteases involved in reshaping the perineuronal net (PNN) and *Mme* encoding for Neprilysin, the enzyme degrading amyloid β-peptides. The pattern of expression of metalloproteases (MPs) was analyzed by single-cell reverse transcriptase multiplex PCR after patch clamp and was compared with the expression of 10 canonical interneurons markers and 12 additional genes from the Allen Atlas. Clustering of these genes by K-means algorithm displays five distinct clusters. Among these five clusters, two fast-spiking interneuron clusters expressing the calcium-binding protein *Pvalb* were identified, one co-expressing *Pvalb* with *Sst* (PV-Sst) and another co-expressing *Pvalb* with three metallopeptidases *Adamts8*, *Adamts15 and Mme* (PV-MP). By using *Wisteria floribunda* agglutinin, a specific marker for PNN, PV-MP interneurons were found surrounded by PNN, whereas the ones expressing Sst, PV-Sst, were not.

Molecular Psychiatry advance online publication, 16 December 2014; doi:10.1038/mp.2014.162

INTRODUCTION

The perineuronal net (PNN) was discovered a century ago by Golgi[1] and rediscovered many times since then.[2] Recent reports have demonstrated the importance of proteases in neuronal plasticity by reshaping the PNN.[3–6] The world of proteases is of paramount importance in biology, and at least 480 genes for proteases have been identified in the whole-mouse genome. In this study, we mined the Allen Mouse Brain *in situ* hybridization (ISH) Atlas for the expression of proteases in cortical interneurons. The Allen Mouse Brain Atlas contains cellular expression patterns of the whole genome in all areas of the mouse brain.[7] In the six layers of the somatosensory cortex, 1043 genes were expressed in various specific neuronal populations, 22 of these genes belonged to the class of protease/peptidases and only 4 proteases/peptidases were expressed preferentially in interneurons (Table 1 and see Supplementary Table S1 in Sorensen *et al.*[8]). These genes are: *Reln* coding for reelin; *Adamts8* and *Adamts15* belonging to the class of metzincin proteases involved in reshaping the PNN and *Mme* encoding for Neprilysin and the enzyme degrading amyloid β-peptides of Alzheimer's plaques.

In recent years, single-cell reverse transcriptase multiplex PCR (scRT-mPCR) after patch clamp has been used to classify cortical interneurons. By using unsupervised clustering expression profiling of canonical interneuronal markers, four classes of GABAergic interneurons were defined: vasoactive intestinal peptide (VIP), neurogliaform (NG), somatostatin (Sst) and fast-spiking parvalbumin (FS-PV).[9–11] In the present work, we have used scRT-mPCR after patch clamp to determine unambiguously in which class of interneurons the four aforementioned proteases were expressed. The clustering was enriched by the addition of 12 genes from the Allen Mouse Brain Atlas selected for being barely or never expressed in excitatory neurons. Adding metallopeptidase genes lead to rearrangement of the FS-PV cluster in two subclusters, one expressing *Sst* (PV-Sst) and another one expressing these three metallopeptidases (PV-MPs), but not *Sst*. It was observed that PV-MP interneurons were surrounded by PNN, whereas PV-Sst were not. These two FS-PV clusters differed also by their electrophysiological properties; the PV-MP neurons discharge at higher frequency and are less excitable than the PV-Sst cluster.

The restricted expression of three metallopeptidases in a subcluster of FS-PV interneurons is intriguing. It is proposed that these secreted proteases modify the structure of the PNN and in turn could be involved in neuronal plasticity and long-term memory.

MATERIALS AND METHODS

Slice preparation

All experiments were performed in accordance with the guidelines of the European Community Council Directive of 24 November 1986 (86/609/EEC). Juvenile C57BL/6 mice (Janvier Labs, Le Genest-Saint-Isle, France) aged postnatal day P14–P17 were deeply anesthetized with halothane and decapitated. Brains were

[1]Centre de Psychiatrie et Neurosciences, Institut National de la Santé et de la Recherche Médicale CPN INSERM U894, Université Paris Descartes, Hôpital Sainte Anne, Paris, France; [2]Allen Institute for Brain Science, Seattle, WA, USA; [3]Department of Psychiatry, Center for Psychiatric Neuroscience, Centre Hospitalier Universitaire Vaudois and University of Lausanne, Prilly-Lausanne, Switzerland and [4]Ecole Supérieure de Physique et de Chimie Industrielles UMR 7637 CNRS-ESPCI, Paris, France. Correspondence: Professor J Rossier, Optogenetics and Brain Imaging, Centre de Psychiatrie et Neurosciences—CPN INSERM U 894—CHSA, 2ter rue d'Alésia, Paris 75014, France
E-mail: jean@rossier.fr
[5]The last three authors are senior authors.
Received 23 January 2014; revised 17 October 2014; accepted 20 October 2014

Table 1. Number of genes detected by ISH in the cerebral cortex

	Entire genome		*Cerebral cortex*		*Interneurons*
Total genes	24 000		1043		120
Peptidases	480	22	*Adam33,* ***Adamts15, Adamts8****, Bace1, Bace2, Capn2, Cyld, Ece2, Klk6,* ***Mme****, Mmp16, Pappa, Pcsk1, Pcsk5, Prss12, Prss23,* ***Reln****, Tfrc, Trhde, Uchl1, Usp11, Usp3*	4	*Adamts15, Adamts8, Mme, Reln*

Abbreviation: ISH, *in situ* hybridization. The 4 metallopeptidases are in bold.

quickly removed and immersed into an ice-cold (~4 °C) slicing solution continuously aerated with carbogen (95% O_2/5% CO_2), containing (in mM): 110 choline chloride, 11.6 sodium ascorbate, 7 $MgCl_2$, 2.5 KCl, 1.25 NaH_2PO_4, 25 glucose, 25 $NaHCO_3$ and 3.1 sodium pyruvate. Chilled brains were placed on the stage of a vibratome and cut into 300-µm-thick slices with a 30–40 ° inclination from the sagittal plane, perpendicular to the surface of the barrel cortex. Slices were subsequently transferred to warm (~33 °C) artificial cerebrospinal fluid solution aerated with carbogen for 20 min and containing (in mM): 126 NaCl, 2.5 KCl, 2 $CaCl_2$, 1 $MgCl_2$, 1.25 NaH_2PO_4, 20 glucose, 26 $NaHCO_3$ and 1 mM of kynurenic acid. Slices were transferred to room temperature for at least 1 h prior to recording. For details see Perrenoud *et al*.[11]

Whole-cell patch-clamp recordings

Slices were submerged in a thermostated recording chamber, placed on the stage of a microscope, equipped with Dodt gradient contrast optics and visualized by infrared illumination. The preparation was continuously superfused (1–2 ml min^{-1}) with oxygenated artificial cerebrospinal fluid warmed to 30 °C. Barrels were visualized in the absence of a light condenser. Pipettes (4–6 MOhms) were pulled from borosillicate capillaries and filled with 8 µl of autoclaved internal solution containing 144 mM K-gluconate, 3 mM $MgCl_2$, 0.5 mM EDTA, 10 mM 4-(2-hydroxyethyl)-1-piperazineethanesulfonic acid, pH 7.2 (285/295 mOsm) and 3 mg ml^{-1} biocytin. Whole-cell patch-clamp recordings were performed at 30 ± 1 °C in current-clamp mode.

scRT-mPCR protocol

At the end of recordings, cellular contents were gently aspirated into the patch pipette. Pipettes were slowly removed from recorded cells to allow for re-closure of the cell membranes. The contents of pipettes were expelled into a microcentrifuge tube in which reverse transcription was performed as described previously.[11] Products of reverse transcription were stored at −80 °C until further processing was performed. The scRT-mPCR protocol was designed to detect the presence of messenger mRNAs coding for 27 genes (26 interneuron genes and *Slc17a7* for vesicular glutamate transporter 1 (VGluT1)). Two successive rounds of amplification were performed using nested primer pairs. All markers were first amplified simultaneously with a first set of primers (Supplementary Table S1), undergoing 21 cycles of amplification (94 °C for 30 s, 60 °C for 30 s and 72 °C for 35 s) in a final volume of 100 µl. Each marker was then amplified individually using a second primer pair internal to the pair used in the first round (nested primer pairs) during 35 additional cycles of amplification. All primers were designed to be on two different exons of the target mRNA, so as to differentiate actual transcripts from eventual genomic DNA contaminations. The presence of products of amplification was finally detected on a 2% agarose gel stained with ethidium bromide.

Electrophysiological analysis

Twenty-eight electrophysiological parameters were measured on traces corresponding to the voltage responses induced by 800-ms hyperpolarizing and depolarizing current pulses. These 28 parameters for 157 cells are available in Supplementary Table S2. Cells were binned into one of four categories based on passive membrane properties, cellular firing properties and anatomical structure visualized under infrared illumination: regular spiking pyramidal, FS, regular spiking nonpyramidal or late spiking (LS), for details see Perrenoud *et al*.[11]

Cluster analysis

Clustering was performed on binarized gene expression values using Ward's hierarchical and K-means using the statistical package R (http://www.r-project.org/). Clustering stability analysis for K-means uses the clustergram to identify optimal k.[12]

Double-fluorescent *in situ* hybridization (dFISH)

Riboprobes were labeled with digoxigenin-UTP and/or dinitrophenyl-11-UTP (DNP; Perkin Elmer, Waltham, MA, USA). A DNP-labeled probe and a digoxigenin-labeled probe were hybridized to the tissue simultaneously. Tyramide signal amplification was performed for each individual probe, using either anti-digoxigenin-horseradish peroxidase with tyramide-biotin, or anti-DNP-horseradish peroxidase with tyramide-DNP. Signals were visualized using streptavidin-Alexa Fluor 488 (Life Technologies-Molecular Probes, Grand Island, NY, USA) and anti-DNP-Alexa Fluor 555 (Life Technologies-Molecular Probes).[13]

Immunofluorescence and confocal imaging

Brain sections of male P40, C57/Bl6 mice, containing S1 were first incubated with phosphate-buffered saline+Triton 0.3%+sodium azide (1 g l^{-1}) containing 2–5% normal horse serum, then placed for 48 h in a solution with a mouse monoclonal anti-parvalbumin (1:2500; Swant, Marly, Switzerland) and a goat anti-somatostatin (1:100; Santa Cruz, Dallas, TX, USA) primary antibody together with the biotin-conjugated lectin *Wisteria floribunda* agglutinin (WFA, 1:2000; Sigma, Buchs, Switzerland). Sections were then washed, incubated with fluorescent secondary antibody conjugates (goat anti-rabbit immunuglobulin (Ig)G (1:300; CY3; Chemicon International, Billerica, MA, USA) and goat anti-mouse (1:300; A488; Life Technologies, Grand Island, NY, USA) and streptavidin 405 conjugate (1:300; Millipore Corporation, Billerica, MA, USA)), when looking at PV, Sst and WFA triple staining. To investigate PV/Sst-MP in the same regions, we used the same immunostaining procedure with a rabbit polyclonal anti-parvalbumin (1:2500; Swant) and an anti-mouse Neprilysin (1:50; R&D Systems, Abingdon, UK) primary antibody together with lectin WFA, counterstained with fluorescent secondary antibody conjugates (goat anti-rabbit IgG (1:300; CY3) and goat anti-mouse (1:300; A488) and fluorescent streptavidin 405 conjugate (1:300)). Sections were similarly stained with a rabbit anti-parvalbumin (1:2500; Swant) and anti-goat ADAMTS8 (1:100; Santa Cruz) primary antibody together with WFA lectin (1:2000), counterstained with fluorescent secondary conjugates (donkey anti-goat IgG (1:500; CY3; Invitrogen, Grand Island, NY, USA) and donkey anti-rabbit IgG (1:500; A488; Invitrogen) and fluorescent streptavidin 405 conjugate (1:300)). Finally, S1 sections were stained

either with a mouse monoclonal anti-parvalbumin (1:2500) or a goat anti-somatostatin (1:100), and a rabbit polyclonal anti-Mybpc1 (1:100; Sigma Life Science, St Louis, MO, USA) together with lectin WFA, then counterstained with fluorescent secondary antibody conjugates (goat anti-mouse (1:300; CY3; Chemicon International) or donkey anti-goat (1:300: CY3) and donkey anti-rabbit (1: 300) and fluorescent streptavidin 405 conjugate (1:300)). Sections were visualized and processed with a Zeiss confocal miscroscope (Feldbach, Switzerland) equipped with x10, x40 and x63 Plan-NEOFLUAR objectives. All peripherals were controlled with LSM 710 Quasar software (Carl Zeiss AG, Feldbach, Switzerland). Z-stacks of nine images (with a 3.13-μm interval) were scanned (1024 × 1024 pixels) with x10 and x63 objectives for analysis qualitative investigation with IMARIS 7.3 software (Bitplane AG, Zurich, Switzerland). A region of interest, as defined in the stereological procedure, was created in the S1. Detailed protocols are available in Cabungcal *et al.*[14,15]

RESULTS

Selection of 27 genes for scRT-mPCR after patch clamp

The genes selected for scRT-mPCR after patch clamp include both novel markers and a number of canonical markers whose products are generally immunodetected in interneurons. These include the two isoforms of glutamate decarboxylase (*Gad1* and *Gad2*), the three calcium-binding proteins, parvalbumin (*Pvalb*), calbindin (*Calb1*) and calretinin (*Calb2*), the four following neuropeptides *Vip*, neuropeptide Y (*Npy*), cholecystokinin, *Sst* and the enzyme nitric oxide synthase 1.[10,11] In two recent large studies using scRT-mPCR after patch clamp these markers delineated four classes of interneurons.[10,11] In the present study, the four protease/peptidases *Adamts15*, *Adamts8*, *Mme* and *Reln* identified by ISH were added (Table 1).

Adamts8 and *Adamts15* are two members of the Metzincin metalloproteinase family, so named for the conserved Met residue at the active site and the use of a zinc ion in the enzymatic reaction. ADAMTSs are acronyms for A Disintegrin And Metalloproteinase with ThromboSpondin motifs.

Mme codes for a peptidase with many aliases: Neprilysin, membrane metalloendopeptidase, neutral endopeptidase, CD10, common acute lymphoblastic leukemia antigen and enkephalinase. Neprilysin is a zinc metalloprotease that degrades a number of secreted peptides, most notably the amyloid β-peptides whose abnormal aggregation causes formation of plaques in Alzheimer's disease. Synthesized as a membrane-bound protein, the Neprilysin ectodomain is released into the extracellular fluid.

Reln codes reelin, an extracellular matrix serine protease. This large extracellular matrix glycoprotein is secreted and regulates neuronal migration.

The other 12 putative markers were selected by analyzing ISH data gene expression in the cerebral cortex. These selected genes are distributed at low density within the laminae of cortex and hippocampus (see Supplementary Table S1 of Sorensen *et al.*[8]) and were rarely or never expressed in excitatory neurons. They are described below in alphabetical order: *Akr1c18*, an aldo-keto reductase involved in the metabolism of progesterone; *Btbd11*, coding a protein with unknown function containing an ankyrin domain and induced by retinoic acid; *Cox6a2*, a subunit of cytochrome *c* oxidase; *Htr3a,* the subunit alpha of the ionotropic serotonin receptor 5HT3A; *Kit*, a proto-oncogene tyrosine-protein kinase; *Mybpc1*, myosin-binding protein C; *Nacc2*, coding Btbd14a, another protein with unknown function; *Nr2f2*, a transcription factor also known as CoupTFII; *Nxph1*, a member of the neurexophilin family that promotes adhesion between dendrites and axons; *Pnoc* pronociceptin, the precursor of the anti-analgesic peptide nociceptin; two semaphorins *Sema4g* and *Sema3c* that act as axonal growth cone guidance molecules. *Slc17a7* encoding the VGluT1 marker for excitatory neurons was chosen as a control.

A scRT-mPCR assay for the simultaneous detection of 27 genes, based on the best possible multiplex set without oligonucleotide cross-reactivity, was developed. List of primers and nested primers are given in the Supplementary Table S1. Neurons (218) from the various layers of somatosensory cortex slices of juvenile mice (P14–17) were patched and analyzed for electrophysiological properties (see Supplementary Table S2). At the end of the recording period, cells were binned between four electrophysiological patterns, regular spiking pyramidal, regular spiking nonpyramidal, FS and LS. The cytoplasm of the neurons was aspirated in the patch pipette and the scRT-mPCR was performed.

Ward's hierarchical clustering

On the basis of binary mRNA expression for the 27 markers, Ward's clustering was performed. Ward's clustering is a hierarchical method that groups cells to maximize the differences between groups and to minimize them within groups. This algorithm identified five groups of neurons (Figure 1a) in agreement with previous findings[10,11] and discriminated excitatory neurons expressing *Slc17a7* from inhibitory neurons expressing *Gad1* and *Gad2*.

The branches of the tree obtained with Ward's hierarchical clustering discriminate interneurons according to their origin. Interneurons from the cortex originate from ganglionic eminence between 11 and 15 days *in utero* and reach the various layers of the cortex for their final maturation. VIP bipolar and NG cells originate from the caudal ganglionic eminence, whereas Sst and PV from the median ganglionic eminence. The large Euclidian distance of the two branches of the tree separating the VIP bipolar and NG clusters from the PV and SOM clusters could reflect the different origins of these clusters. In a recent publication, Scanziani *et al.*[16] have identified similar clusters.

Both VIP and NG clusters were enriched for the two genes *Kit* and *Sema3c*. These genes were barely expressed in other clusters. *Kit and Sema3c* define a single cluster of cells named hereunder KS. The Ward's algorithm indicated also that PV cells could be divided in two different clusters based on the expression of the 27 selected molecular markers. Other clustering algorithms, that is, affinity propagation and K-means were tested. The K-means, a non-hierarchical algorithm, resulted in a more refined partition of PV interneurons.

K-means clustering

As shown, in Figure 1b, the cluster stability analysis showed that a K-means value of 6 ($k = 6$) provided the best separation between clusters. Similarly with the Ward's clustering, the KS cluster (yellow in Figure 1a) was subclustered in two subclasses, one (KS-VIP in green) expressing *Vip* with no expression of *Nxph1,* and another one, KS-NG (orange in Figure 1a) that does not express *Vip* but expresses *Nxph1* at a relatively high occurrence (17/35). This latter subcluster contains 40% of LS neurons characterized by a delay to generate action potentials (Supplementary Table S2). LS firing pattern is the electrophysiological signature of NG cells[9] and was never observed in cells from other clusters.

Recently, it was proposed that PV basket cells could be subdivided in four classes according to their electrophysiological properties.[17] Figure 1a indicates that the K-means algorithm with a *k* of 6, now dissociates the PV cluster in two subclusters. A PV subcluster co-expresses *Pvalb* and *Sst*. This cluster was labeled PV-Sst in Figure 1a and highlighted in purple. The other PV cluster expresses *Pvalb* and the three metallopeptidases *Mme*, *Adamts8* and *Adamts15*. This cluster was labeled PV-MP and highlighted in blue in Figure 1a. The three metallopeptidases were not or very rarely expressed in the five other clusters.

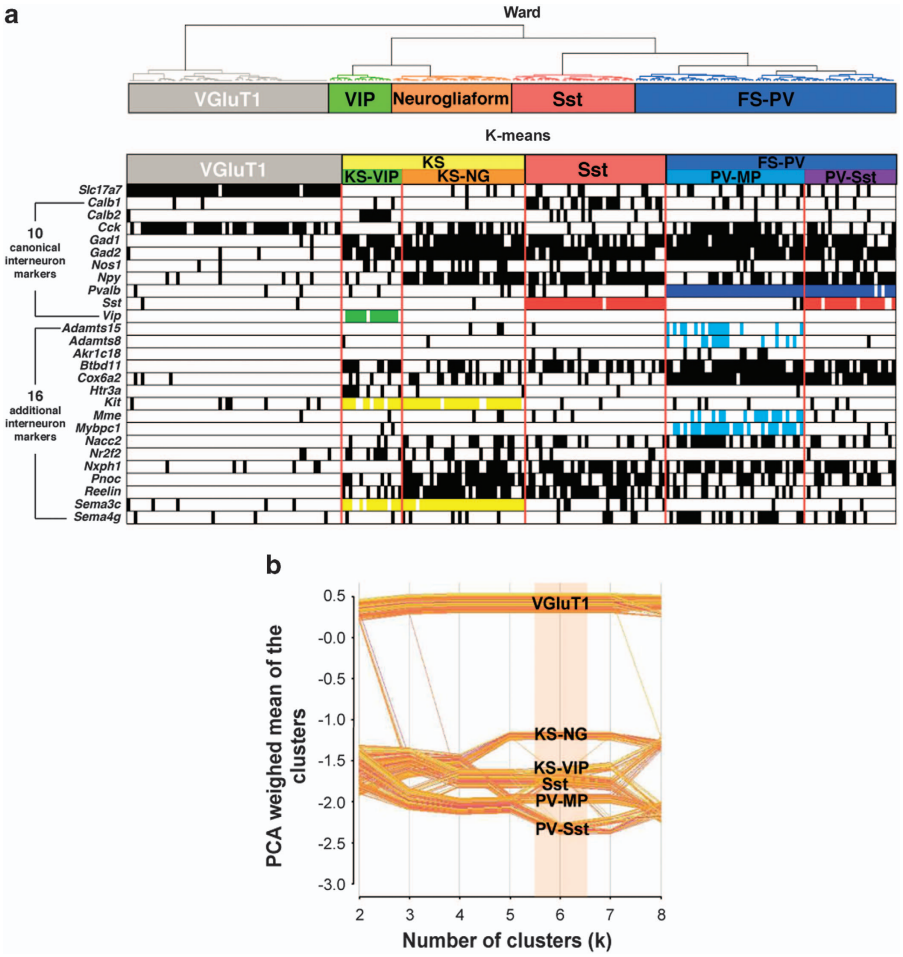

Figure 1. Clustering of 218 neurons in five (Ward) or six (*K*-means) classes by gene expression. Each individual cell from the somatosensory cortex of 15–19-day-old mice is represented along the x-axis. In each of the 218 columns, detection of a gene by scRTmPCR in a single neuron is indicated by black or colored squares. The list of 27 genes detected is on the y-axis. Anatomical and electrophysiological profiles of most of these cells have been described previously.[11] Complete data are in Supplementary Table S2. (**a**) Ward's hierarchical and *K*-means ($k=6$) clustering for the presence or absence (binarization) of gene expression only. The electrophysiological profiles from Supplementary Table S2 were not used for the clustering. (**b**) Cluster stability analysis based on principal component analysis (PCA).[12] FS-PV, fast-spiking parvalbumin; KS, c-Kit with semaphorin3c; NG, neurogliaform; PV-MP, parvalbumin with metallopeptidases; PV-Sst, parvalbumin with somatostatin; Sst, somatostatin; VGluT1, vesicular glutamate transporter 1; VIP, vasoactive intestinal peptide.

Table 2. Differences in electrophysiological properties of PV-MP and PV-Sst cortical interneurons

	PV-MP (n = *39*)	*PV-Sst* (n = *26*)
Passive membrane property		
Input resislance (MΩ)	224.9 ± 19.9 PV-MP≪ PV-Sst	337.9 ± 36.9
Above threshold properties		
Rheobase (pA)	146.9 ± 16.1 PV-MP > PV-Sst	91.9 ± 15.4
Maximal frequency (Hz)	182.9 ± 6.8 PV-MP⋙PV-Sst	148.4 ± 7.5

Abbreviations: PV-MP, parvalbumin with metallopeptidase; PV-Sst, parvalbumin with somatostatin. Values are weighted means ± s.e.m.; *n*, number of cells. < *P* below 0.05, ≪ *P* below 0.005, ⋘ *P* below 0.001.

Subclustering of FS-PV cells

The comparison between Ward's and K-means algorithms resulted in a distribution that is highly similar for VGluT1, KS-VIP, KS-NG and Sst clusters. On the other hand, K-means algorithm reveals two subclasses of PV cells, PV-MP and PV-Sst. Neurons from both PV subclusters display a maximal discharge frequency >130 Hz (Table 2), a feature typical of FS-PV cells.[9] The high-frequency firing pattern of FS-PV cells utilizes maximal mitochondrial oxidative capacity and may account for the detection of the respiration chain gene *Cox6a2* found in most of the cells within PV-MP and PV-Sst clusters. When looking at their electrophysiological properties, these two subclasses of FS-PV displayed different characteristics: the 39 PV-MP cells discharge at a higher maximal frequency than the 26 PV-Sst cells but are on average, less excitable due to their lower mean input resistance and higher rheobase values (Table 2).

These two PV clusters are also different in the expression of five genes: *Akr1c18*, *Mybpc1*, *Mme*, *Adamts8* and *Adamts15* are expressed in PV-MP cluster and seldom expressed or neither in PV-Sst cluster nor in the other clusters of inhibitory or excitatory neurons. *Akr1c18* codes for an enzyme of steroid metabolism; *Mybpc1* for myosin-binding protein C and *Mme* for the zinc metallopeptidase Neprilysin, whereas *Adamts8* and *Adamts15* are two metallopeptidases that could cleave the proteoglycans aggrecan and versican, two major components of the extracellular

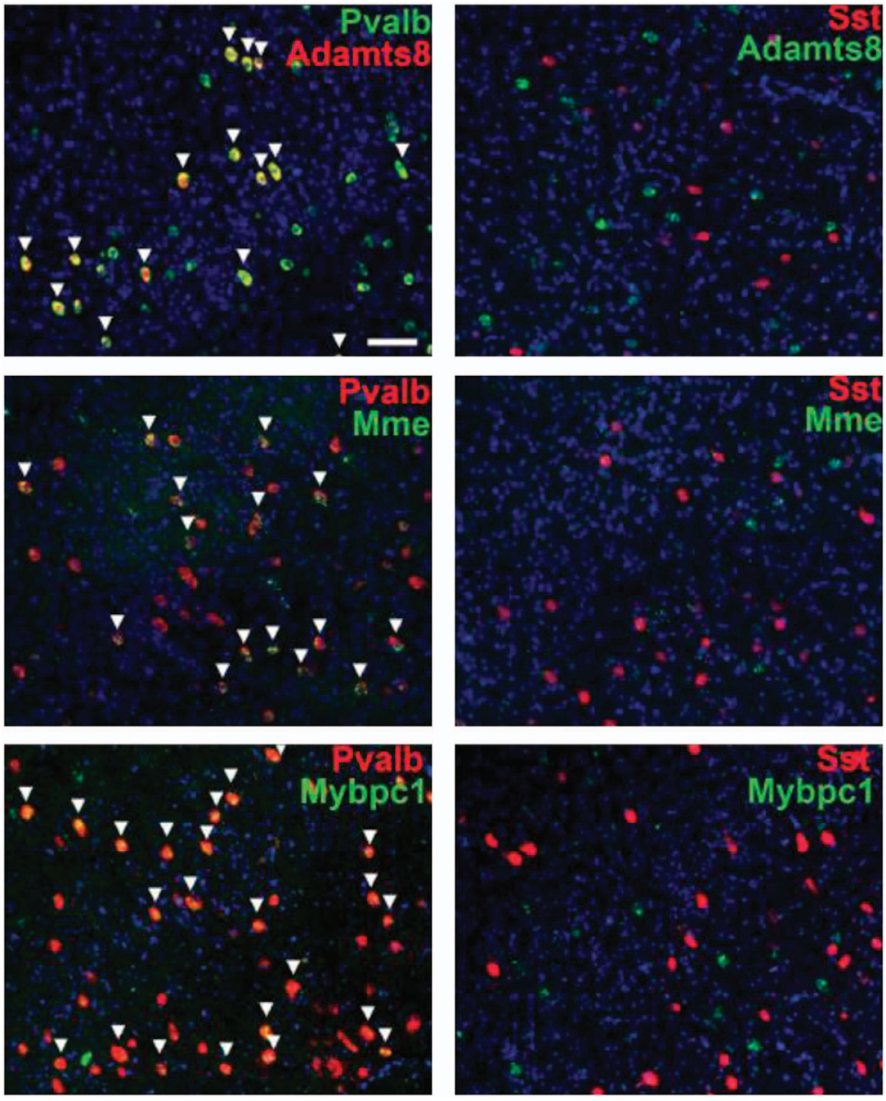

Figure 2. Double-fluorescent *in situ* hybridization (dFISH). On the left, arrows indicate neurons co-expressing *Adamts8, Mme and Mybpc1* with *Pvalb*. On the right, *Sst* is not associated with expression of *Adamts8, Mme and Mybpc1*. Somatosensory cortex of 58-day-old mice. Bar 30 micron. Sst, somatostatin.

matrix of the PNN.[18,19] *Adamts8* and *Adamts15* were also identified previously in FS-PV interneurons by Nelson *et al*.[20] Expression of *Mybpc1, Mme, Adamts8* and *Adamts15* is highlighted in pale blue in the PV-MP cluster (Figure 1a). *Mybpc1* was detected in most of the cells of the PV-MP cluster (26/39) and could be considered as a surrogate marker of the PV-MP cluster.

dFISH analysis of *Mybpc1, Mme, Adamts8* and *Adamts15* with *Pvalb* was performed and confirms that mRNA for *Mybpc1* and for the three MPs are coexpressed with *Pvalb* in all layers of the somatosensory cortex. Figure 2 compares dFISH of *Pvalb* or *Sst* with *Adamts8, Mme and Mybpc1*. Colocalization was found for *Pvalb* and *Adamts8* (red), *Mme* (green) *and Mybpc1* (green) on the other hand these three genes (all three in green) were never colocalized with *Sst* (red). These dFISH results obtained in P58 adult mice are in agreement with the scRT-mPCR results obtained with juvenile mice in Figure 1a.

The colocalization of the MPs and Mybpc1 with PV was further investigated at the protein level by triple-staining, double-immunohistochemistry coupled with WFA biotin streptavidin. WFA labels specifically the PNN. In Figure 3, the WFA lectin is always colored in blue. In Figures 3b–d, antibodies against ADAMTS8, Mme (Neprilysin) and Mybpc1 indicate that these markers are colocalized with PV and also with WFA. Figure 3e indicates that Sst (red) is not colocalized with Mybpc1 (green) nor with WFA. Figure 3a presents the triple staining of PV, Sst and WFA. The higher magnification exhibits four PV cells stained in red; one cell (upper middle) displays PV and WFA without Sst; two cells (upper left and middle left) show PV and Sst without WFA; one cell (middle left) with PV, Sst and WFA. At high magnification it was often observed that projections of PV and Sst immunoreactivities were basket like. In the Supplementary Figure S1, panel A shows that PV-stained cells are frequently, but not always, associated with WFA, on the other hand panel B shows that Sst is not associated with WFA.

Supplementary Figure S2 shows with triple immunostaining that the two metallopeptidases *ADAMTS8* and *Mme* are colocalized in the same PV interneurons. Analysis of Figure 1 and Supplementary Table 2 indicates that simultaneous detection by RT-PCR of the three genes *Adamts8*, *Adamts15* and *Mme* was found in 4 cells over the 39 cells of the cluster PV-MP; simultaneous detection

of two genes among the three peptidases was found in 10 cells over 39. Overall, multiple immunostainings and scRT-mPCRs indicate that the presence of one of the three metallopeptidases is not excluding the presence of the two others.

The general conclusions of the ISH and immunocytological studies are that two classes of PV basket interneurons were identified in the somatosensory cortex of the adult mouse: PV interneurons expressing MP were surrounded by PNN and PV expressing Sst were not enwrapped by PNN. The generalization of this observation to other areas of the cortex remains to be done.

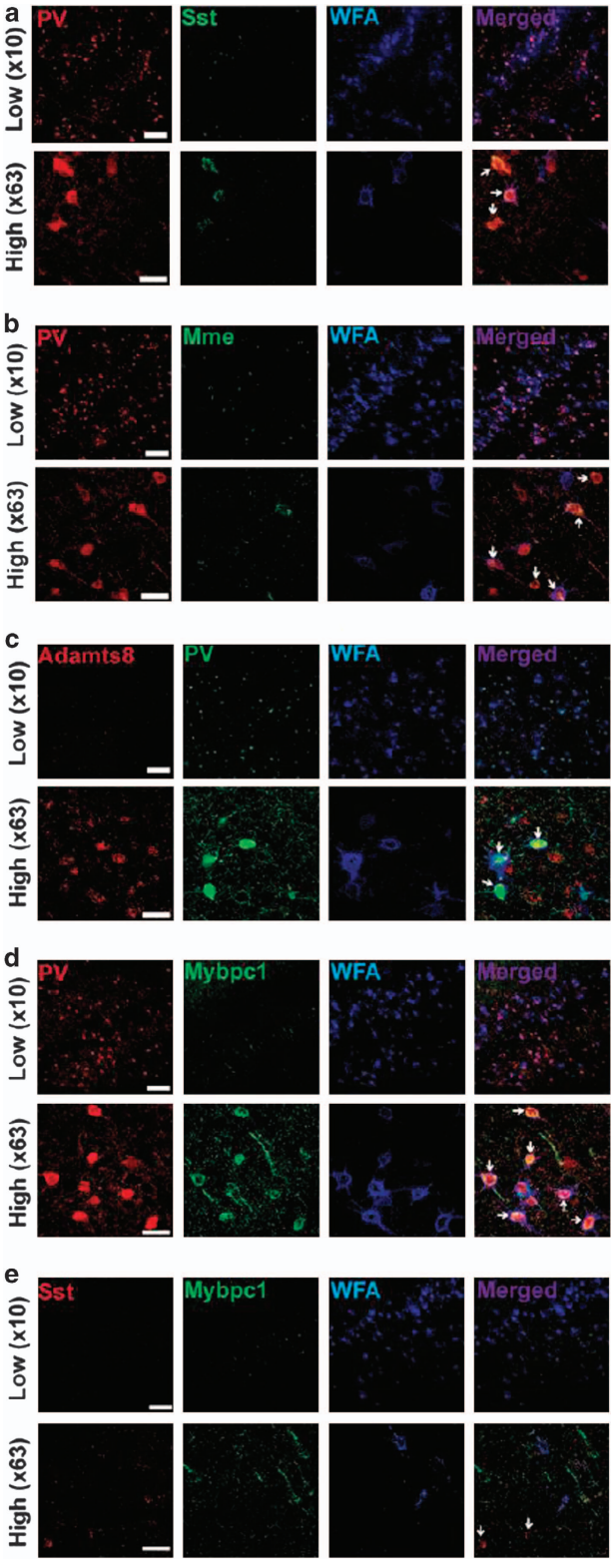

Figure 3. Immunofluorescence and confocal imaging. Parvalbumin (PV) interneurons enwrapped with perineuronal net contain metallopeptidase protein. Colocalization of PV, somatostatin (Sst), *Wisteria floribunda* agglutinin (WFA), Mme (Neprilysin), Adamts8 and Mybpc1. (**a**) Micrograph of parvalbumin interneurons (red) revealing that most PV coexpressed with Sst (green) are void of perineuronal net (WFA; blue). (**b**) Parvalbumin interneurons (red) enwrapped with perineuronal net (blue) contain Neprilysin (Mme; green). (**c**) Adamts8 (red) can be found in all parvalbumin interneurons (green), but not exclusively. (**d**) The majority of parvalbumin interneurons (red) enwrapped by perineuronal net (blue) colocalize with Mybpc1 (green). (**e**) Somatostatin-positive neurons (red) are not enwrapped by perineuronal net (WFA, blue) and do not colocalize with Mybpc1 (green). Scale bar, 80 μm in low (×10) and 30 μm in high (×63) magnification. Arrows depicts main cell of interests (red). This observation was confirmed in three male 40-day-old C57/Bl6 mice.

DISCUSSION

In this report, the pattern of expression of four proteases by cortical interneurons was analyzed by scRT-mPCR after patch clamp and was compared with the expression of 23 additional genes. Clustering of these genes by K-means algorithm displays five distinct clusters. Among these five clusters, two FS interneuron clusters expressing the calcium-binding protein *Pvalb* were identified: one PV-Sst co-expressing *Pvalb* with *Sst* and another PV-MP co-expressing *Pvalb* with three metallopeptidases *Adamts8, Adamts15 and Mme*. By using WFA, a specific marker for PNN, PV-MP interneurons were found surrounded by PNN, whereas interneurons expressing Sst and PV-Sst were not.

New markers delineating cell clusters

The 27 markers used in scRT-mPCR defined five clusters. Two clusters co-express two molecular markers: tyrosine-protein kinase *Kit* (44/52) and semaphorin growth cone guidance molecule *Sema3c* (47/52). This KS cluster was subclustered in a KS-VIP cluster (17 cells) and in a KS-NG cluster (35 cells). According to previous developmental studies, these two clusters, KS-VIP and KS-NG contain cells originating mainly in the caudal ganglionic eminence.[9]

The KS-VIP cluster expressed with high occurrence *Vip* (14/17), calretinin (*Calb2*) (9/17) and ionotropic serotonin receptor subunit *Htr3a* (8/17). *Vip* was not expressed in the other clusters.

The KS-NG cluster expressed glycoprotein serine protease reelin *Reln* (28/35) and the precursor of the anti-analgesic peptide, pronociceptin *Pnoc* (30/35). The KS-NG cluster contains 40% of neurons with LS firing pattern characterized by a delay to generate action potentials (Supplementary Table S2). The LS firing pattern is the electrophysiological signature of NG cells[9] and was never observed in cells from other clusters. *Npy* was detected in 31 of the 35 cells of that cluster but was also detected at high occurrence in Sst, PV-MP and PV-Sst clusters, confirming that *Npy* is not a specific marker for NG cells.[11]

Sst cluster expresses *Sst* (39/40), *Calb1* (23/40) and *Npy* (34/40). Sst and FS-PV interneurons have both their embryonic origin in the medial ganglionic eminence and share many features.[21]

On anatomical and electrophysiological criteria, two main classes of FS-PV interneurons have previously been identified, chandelier cells that target the proximal segment of pyramids and basket cells that target soma and proximal dendrites of pyramids.[9]

In this work as well as in previous works[10,11] chandelier interneurons[22] were not identified on the slice preparations.

In this study, *Slc17a7* (VGluT1), the canonical marker for excitatory neurons, was detected in almost 20% of the interneurons. This was not unexpected as the coexistence of vesicular transporters for glutamate and GABA in synaptic vesicles of GABAergic neurons was already reported.[23] Our observation gives more grounds to the possibility that subpopulations of GABAergic interneurons could release glutamate making a possible fine-tuning between inhibitory and excitatory output.[24]

The originality of this work was indeed the discovery of two distinct clusters of FS-PV cells that display different electrophysiological profiles and express different subsets of genes. The cells in the PV-Sst cluster expressing both *Pvalb* and *Sst* are more excitable and discharge at a lower frequency than the cells in the PV-MP cluster (Table 2). This latter cluster expresses the three peptidases and also *Mybpc1* whose role in this cluster is still unknown.

Reshaping the PNN by ADAMTS and Neprilysin secreted by PV-MP interneurons

The expression of peptidases within a subpopulation of FS-PV interneurons could have important physiological consequences. The importance of PNN in the critical period determining ocular dominance has been highlighted already in 2002 by Pizzorusso *et al*.[25] They have shown that reshaping the extracellular PNN by destroying its major constituents, chondroitine sulfate proteoglycans with chondroitinase-ABC, had a marked effect in prolonging the critical period of ocular dominance in the visual system. More recently, peptidases have been recognized to be important actors in neuronal plasticity.[3] The number, location and identification of the various peptidases involved in plasticity are not yet well characterized. Good candidates are the very large family of Metzincin proteases, with matrix metalloproteinases (MMP), ADAM and ADAMTS. These latter enzymes are secreted in the extracellular fluid. The gene family of *Adamts* is large with 19 members that can be divided in four major subfamilies. Both *Adamts8* and *Adamts15* expressed in FS-PV interneurons are members of the subfamily A. Members of this family cleave the major cartilage proteoglycans aggrecan and versican, two major components of the PNN.[4]

Among the >20 MMPs, MMP9 has been particularly studied and found to be important for the establishment of late long-term potentiation.[5,26] The current hypothesis would be that MMP9 in CA1 of the hippocampus modifies the shape and the organization of dendritic spines. In the present study, MMP9 was not detected in the somatosensory cortex. Our observation that a subclass of FS-PV interneurons enwrapped in the PNN expresses three MPs led us to propose that these secreted MPs could reshape the proteoglycans of the PNN. Reshaping the PNN is at the grounds of the recent proposal of Tsien[6] that very long-term memories could be stored in the pattern of holes in the PNN.

On the roles of metallopeptidases in Alzheimer's disease

The specific expression of *Mme* in a subpopulation of FS-PV interneurons could have considerable interest for Alzheimer's disease. *Mme* codes the zinc metallopeptidase Neprilysin. This enzyme is considered as a major β-amyloid-degrading enzyme. Ten years ago, Iwata *et al.*[27] had observed that Neprilysin was downregulated in aging and Alzheimer's disease.[27] In turn, several attempts have been made to upregulate its endogeneous production as a possible therapeutic target for Alzheimer's disease.[28]

The present observation that in the cerebral cortex Neprilysin is expressed in a subcluster of FS-PV interneurons should stimulate new genetic or pharmacological investigations aiming at the increase of Neprilysin production by this restricted subclass of interneurons. FS-PV interneurons are at the origin of gamma oscillation in the cortex and contribute to cognitive functions.[29,30] A prevalent hypothesis is that cognitive deficits in Alzheimer's disease are associated with altered activities of FS-PV interneurons.[31] Restoring viability of FS-PV interneurons and increasing their production of Neprilysin may become an accessible target for the treatment of the cognitive deficits in Alzheimer's disease.

On the importance of PNN in schizophrenia

Lewis *et al.*[32,33] have also associated cognitive dysfunction in schizophrenia with altered inputs on FS-PV interneurons. The importance of the PNN in schizophrenia was highlighted recently by Beretta.[34,35] Anatomo-pathology from patients suffering from schizophrenia has demonstrated that PNN is altered in the cortex of these patients. On the other hand it was observed in mice that PNN protects FS-PV interneurons against oxidative stress.[14,15]

In this report, we show by using WFA, a specific marker for PNN, that PV-MP interneurons are surrounded by PNN, whereas the one expressing Sst, PV-Sst, were not. It thus seems plausible that PV-Sst interneurons not protected by PNN are a distinct class of FS-PV interneurons highly susceptible to oxidative stress induced by developmental insults in schizophrenia.[36]

CONFLICT OF INTEREST

The authors declare no conflict of interest.

ACKNOWLEDGMENTS

We wish to thank Hélène Geoffroy for assistance in scRT-mPCR, Aline Monin for her help with immunolocalization and Staci Sorensen for her help in defining molecular markers of cortical interneurons. We thank the Allen Institute founders, Paul G Allen and Jody Patton, for their vision, encouragement and support. We are grateful for the professional support of the entire Atlas production team and the Information Technology team at the Allen Institute. This work was supported by grants from Agence Nationale de la Recherche, Paris, France (grant ANR SVSE 4 Brainvasc, ANR TECSAN VSDIR) and Fondation Pour les Sciences du Cerveau to JR and grants from Swiss National Science Foundation (# 310030_135736/1, National Center of Competence in Research 'SYNAPSY - The Synaptic Bases Of Mental Diseases', 51AU40_125759) and the Avina, Damm-Etienne and Alamaya Foundations to KD.

REFERENCES

1 Golgi C. Intorno alle strutture delle cellule nervosa. Bolletino della Societa medico-chirurgica di Pavia 1898; Seduta del 19 Aprile: 1-14.
2 Celio MR, Spreafico R, De Biasi S, Vitellaro-Zuccarello L. Perineuronal nets: past and present. *Trends Neurosci* 1998; **21**: 510–515.
3 Huntley GW. Synaptic circuit remodelling by matrix metalloproteinases in health and disease. *Nat Rev Neurosci* 2012; **13**: 743–757.
4 Wang D, Fawcett J. The perineuronal net and the control of CNS plasticity. *Cell Tissue Res* 2012; **349**: 147–160.
5 Rivera S, Khrestchatisky M, Kaczmarek L, Rosenberg GA, Jaworski DM. Metzincin proteases and their inhibitors: foes or friends in nervous system physiology? *J Neurosci* 2010; **30**: 15337–15357.
6 Tsien RY. Very long-term memories may be stored in the pattern of holes in the perineuronal net. *Proc Natl Acad Sci USA* 2013; **110**: 12456–12461.
7 Lein ES, Hawrylycz MJ, Ao N, Ayres M, Bensinger A, Bernard A *et al.* Genome-wide atlas of gene expression in the adult mouse brain. *Nature* 2007; **445**: 168–176.
8 Sorensen SA, Bernard A, Menon V, Royall JJ, Glattfelder KJ, Desta T *et al.* Correlated gene expression and target specificity demonstrate excitatory projection neuron diversity. *Cereb Cortex* 2013; doi: 10.1093/cercor/bht243 (e-pub ahead of print).
9 Ascoli GA, Alonso-Nanclares L, Anderson SA, Barrionuevo G, Benavides-Piccione R, Burkhalter A *et al.* Petilla terminology: nomenclature of features of GABAergic interneurons of the cerebral cortex. *Nat Rev Neurosci* 2008; **9**: 557–568.
10 Karagiannis A, Gallopin T, Dávid C, Battaglia D, Geoffroy H, Rossier J *et al.* Classification of NPY-expressing neocortical interneurons. *J Neurosci* 2009; **29**: 3642–3659.
11 Perrenoud Q, Rossier J, Geoffroy H, Vitalis T, Gallopin T.. Diversity of GABAergic interneurons in layer VIa and VIb of mouse barrel cortex. *Cereb Cortex* 2013; **23**: 423–441.

12 Schönlau M. The clustergram: a graph for visualizing hierarchical and non-hierarchical cluster analyses. *Stata J* 2002; **2**: 391–402.
13 Thompson CL, Pathak SD, Jeromin A, Ng LL, MacPherson CR, Mortrud MT *et al.* Genomic anatomy of the hippocampus. *Neuron* 2008; **60**: 1010–1021.
14 Cabungcal JH, Steullet P, Morishita H, Kraftsik R, Cuenod M, Hensch TK *et al.* Perineuronal nets protect fast-spiking interneurons against oxidative stress. *Proc Natl Acad Sci USA* 2013; **110**: 9130–9135.
15 Cabungcal JH, Steullet P, Kraftsik R, Cuenod M, Do KQ. Early-life insults impair parvalbumin interneurons via oxidative stress: reversal by N-acetylcysteine. *Biol Psychiatry* 2013; **73**: 574–582.
16 Pfeffer CN, Xue M, He M, Huang ZJ, Scanziani M. Inhibition of inhibition in visual cortex: the logic of connections between molecularly distinct interneurons. *Nat Neurosci* 2013; **16**: 1068–1076.
17 Helm J, Akgul G, Wollmuth LP. Subgroups of parvalbumin-expressing interneurons in layers 2/3 of the visual cortex. *J Neurophysiol* 2013; **109**: 1600–1613.
18 Giamanco KA, Matthews RT. Deconstructing the perineuronal net: cellular contributions and molecular composition of the neuronal extracellular matrix. *Neuroscience* 2012; **218**: 367–384.
19 Brocker CN, Vasiliou V, Nebert DW. Evolutionary divergence and functions of the ADAM and ADAMTS gene families. *Hum Genomics* 2009; **4**: 43–55.
20 Okaty BW, Miller MN, Sugino K, Hempel CM, Nelson SB. Transcriptional and electrophysiological maturation of neocortical fast-spiking GABAergic interneurons. *J Neurosci* 2009; **29**: 7040–7052.
21 Rudy B, Fishell G, Lee S, Hjerling-Leffler J. Three groups of interneurons account for nearly 100% of neocortical GABAergic neurons. *Dev Neurobiol* 2011; **71**: 45–61.
22 Taniguchi H, Lu J, Huang ZJ. The spatial and temporal origin of chandelier cells in mouse neocortex. *Science* 2013; **339**: 70–74.
23 Fattorini G, Verderio C, Melone M, Giovedì S, Benfenati F, Matteoli *et al.* VGLUT1 and VGAT are sorted to the same population of synaptic vesicles in subsets of cortical axon terminals. *J Neurochem* 2009; **110**: 1538–1546.
24 Zander JF, Münster-Wandowski A, Brunk I, Pahner I, Gómez-Lira G, Heinemann U *et al.* Synaptic and vesicular coexistence of VGLUT and VGAT in selected excitatory and inhibitory synapses. *J Neurosci* 2010; **30**: 7634–7645.
25 Pizzorusso T, Medini P, Berardi N, Chierzi S, Fawcett JW, Maffei L. Reactivation of ocular dominance plasticity in the adult visual cortex. *Science* 2002; **298**: 1248–1251.
26 Nagy V, Bozdagi O, Matynia A, Balcerzyk M, Okulski P, Dzwonek J *et al.* Matrix metalloproteinase-9 is required for hippocampal late-phase long-term potentiation and memory. *J Neurosci* 2006; **26**: 1923–1934.
27 Iwata N, Tsubuki S, Takaki Y, Shirotani K, Lu B, Gerard NP *et al.* Metabolic regulation of brain Abeta by neprilysin. *Science* 2001; **292**: 1550–1552.
28 Nalivaeva NN, Belyaev ND, Zhuravin IA, Turner AJ. The Alzheimer's amyloid-degrading peptidase, neprilysin: can we control it?. *Int J Alzheimers Dis* 2012; **2012**: 383796.
29 Cardin JA, Carlén M, Meletis K, Knoblich U, Zhang F, Deisseroth K *et al.* Driving fast-spiking cells induces gamma rhythm and controls sensory responses. *Nature* 2009; **459**: 663–667.
30 Sohal VS, Zhang F, Yizhar O, Deisseroth K.. Parvalbumin neurons and gamma rhythms enhance cortical circuit performance. *Nature* 2009; **459**: 698–702.
31 Verret L, Mann EO, Hang GB, Barth AM, Cobos I, Ho K *et al.* Inhibitory interneuron deficit links altered network activity and cognitive dysfunction in Alzheimer model. *Cell* 2012; **149**: 708–721.
32 Glausier JR, Fish KN, Lewis DA.. Altered parvalbumin basket cell inputs in the dorsolateral prefrontal cortex of schizophrenia subjects. *Mol Psychiatry* 2014; **19**: 57–67.
33 Lewis DA, Curley AA, Glausier JR, Volk DW.. Cortical parvalbumin interneurons and cognitive dysfunction in schizophrenia. *Trends Neurosci* 2011; **35**: 57–67.
34 Berretta S. Extracellular matrix abnormalities in schizophrenia. *Neuropharmacology* 2012; **62**: 1584–1597.
35 Mauney SA, Athanas KM, Pantazopoulos H, Shaskan N, Passeri E, Berretta S *et al.* Developmental pattern of perineuronal nets in the human prefrontal cortex and their deficit in schizophrenia. *Biol Psychiatry* 2013; **74**: 427–435.
36 Steullet P, Cabungcal JH, Monin A, Dwir D, O'Donnell P, Cuénod *et al.* Redox dysregulation, neuroinflammation, and NMDA receptor hypofunction: a "central hub" in schizophrenia pathophysiology? *Schizophr Res* 2014; doi: 10.1016/j.schres.2014.06.021 (e-pub ahead of print).

Supplementary Information accompanies the paper on the Molecular Psychiatry website (http://www.nature.com/mp)